# Screening Effects When Sampling Suspensions in Laminar Flow through Pores

**Francis J. Jones and Charles B. Weinberger**
Dept. of Chemical Engineering, Drexel University, Philadelphia, PA 19104

*Dilute suspensions of neutrally buoyant, uniform-diameter spheres in a viscous liquid are sampled through pores in the wall of a stirred tank. These studies are performed to investigate screening effects near the sampling orifice that cause samples to be deficient in solids. The ratio of sphere concentration in the sample to that of the original suspension ranges from 0.08 to 1.12. Sample concentration decreases with decreasing sampling pore diameter and increasing stirring rates. The objectives of this work are both to obtain experimental relationships and to develop predictive techniques relating flow fields to sample concentration.*

*Sample concentration is predicted by calculating particle trajectories in the region near the pore and by accounting for steric exclusion. Particle trajectories can differ from fluid streamlines due to lift forces generated in the flow field. These estimates constitute a priori predictions, since they do not rely on or introduce any empirical parameters. Predicted values of sample concentrations agree closely with data.*

## Introduction

Understanding the flow behavior of suspensions in the vicinity of a pore is important both to membrane separation and to sampling. Typically, a particle-filled liquid suspension entering a pore is deficient in particles, relative to the original suspensions, due to screening effects at the pore. If one attempts to sample the suspension, this means that the sample's concentration will be too low. Similarly, if one uses a porous membrane to concentrate suspensions and the pores are slightly larger than the particles, the separation effectiveness will be better than expected. Such screening can occur both in turbulent (Nasr, 1986) and in laminar flow. Our focus is restricted to suspensions in laminar flow.

Fahraeus (1929), in a study of blood viscosity, found that blood samples taken from a tank through a thin glass tube contained fewer red cells per volume than the blood in the tank. Expressing $\phi_t$ as the volume concentration of particles in the bulk and $\phi_s$ as the concentration in the sample, Fahraeus found that the dimensionless relative sample concentration, $\Phi_s$:

$$\Phi_s = \phi_s/\phi_t < 1. \tag{1}$$

Further, the concentration "deficiency" grew as the sampling tube's inner diameter was decreased. Near the heart, blood contains approximately 40 vol. % red blood cells. In small capillaries, far away from the heart, red cell concentration decreases to about 10 vol. %. It is thought that the decrease in red cells is due to a screening effect at the entrance to branch (generally smaller) vessels. This is frequently referred to as the "Fahraeus effect." Therefore, $\Phi_s$ depends on the relative size of the pore; as $d/2a$, the ratio of pore diameter to particle diameter, decreases toward unity, the effect becomes more pronounced.

In addition to pore diameter, one would also expect the velocity field in the vicinity of the sampling pore to affect the concentration deficiency. A suitable independent variable here could be $V_{ch}/V_s$, or some characteristic velocity dedimensionalized by an average velocity in the pore. One might expect small characteristic or suspension velocity and high sampling velocity to yield truer, or less-concentration-deficient, samples. This is indeed the case for samples taken in turbulent velocity fields as in Nasr, but little experimental work has been reported for laminar velocity fields. Fahraeus did not describe this velocity field and neither did more recent experimental investigators (Cokelet, 1976; Gaehtgens, 1980). The objectives of the experimental phase of the present work are to determine the dependence of the relative

Correspondence concerning this article should be addressed to F. J. Jones.
Current address of F. J. Jones: Department of Chemical Engineering, Louisiana Tech. University, Ruston, LA 71272.

sample concentration $\Phi_s$ on both the relative pore size, $d/a$, and the dimensionless velocity field, $V_{ch}/V_s$, at the sampling pore. Certain independent variables, including particle density, particle sphericity, particle size distribution, and particle concentration, are avoided intentionally by using neutrally buoyant spheres of a single size in dilute concentration.

In addition to the experimental phase of the work, it is important to determine whether the functional dependence of $\Phi_s$ on $d/a$ and $V_{ch}/V_s$ can be predicted *a priori*. Yan et al. (1991) explained the screening of red cells based on the hydrodynamic interactions that occur in creeping flow ($Re \ll 0.1$). Dagan et al. (1982, 1983) describe, mathematically, hydrodynamic interactions of spherical particles with a wall containing a sampling port in creeping flow. The work of Dagan and Yan was restricted to very slow flow, where there are no inertial effects. However, the creeping-flow equations eliminate the inertial terms of the Navier–Stokes equations and hence the possibility of calculating any lateral (inertial) migration (Bretherton, 1962). Our experiments also include laminar flow, but with velocities sufficient to render inertial effects not negligible.

Lateral particle migration, which can lead to a diminution of $\Phi_s$, corresponds to the case of a particle crossing over streamlines of a fluid suspension. This sort of particle migration is well documented. Segre and Silberberg (1961, 1962a,b) performed an experimental investigation of dilute suspensions of neutrally buoyant particles in Poiseiulle flow in tubes with tube Reynolds numbers ranging from about 3 to 700. They found that, although the liquid was undergoing essentially rectilinear motion, particles flowing along with the fluid migrate either away from the wall or away from the center line, ultimately forming, well downstream, a thin annular ring about 0.6 of the way from the center line to the wall. This phenomenon is called the "tubular pinch effect." This migration is also known as "inertial migration" (Bretherton, 1962) or, simply, "lift."

The lateral migration of neutrally buoyant spheres has since been theoretically investigated by Cox and Brenner (1968), Ho and Leal (1974), and Vasseur and Cox (1976), among others. Schonberg and Hinch (1989) described, mathematically, the tubular pinch effect in the experiments of Segre and Silberberg (1962a,b), albeit for parabolic flow between parallel plates rather than in a tube. They used singular perturbation expansions to calculate lateral migration with a channel Reynolds number range of 1 to 150. Their results are summarized in plots of dedimensionalized lateral migration velocity vs. position, which allows one to calculate lateral migration velocities, depending on particle size, channel size, fluid velocity, and location.

Many engineering problems may be explained by a lateral migration mechanism. Green and Belfort (1980) and Altena and Belfort (1984) describe activity at the surface of a cross-flow membrane where solutions of macromolecules have filtration rates an order of magnitude lower than colloidal particles. This is called the "flux paradox" since the much larger colloidal particles would be expected to clog the membrane faster. This can be explained by considering macromolecules as part of the fluid continuum and therefore hydrodynamically inactive. However, large solid particles cannot deform in a shear field as an equivalent element of fluid would and therefore cause a disturbance flow (hydrodynamic activity). If this disturbance flow interacts with a nearby wall/membrane, the particle migrates away from it. Hence, under proper flow conditions, particles migrate away from the membrane, decreasing fouling rates. This idea is experimentally reinforced by Otis et al. (1986). Later, Levesley and Bellhouse (1993) separated particles in a cross-flow membrane system according to size due to the different balance between lift and drag forces.

Berge (1990) has measured lateral migration in tubes as small as 30 microns in diameter. Also, Bauser et al. (1982) has observed the tubular pinch effect for blood flowing in a tube (with a membrane wall) with a diameter of 225 microns and a tube Reynolds number of approximately 0.004. Therefore, lateral migration is a plausible mechanism for the screening of red cells at microvessel bifurcations. It is also a plausible mechanism for screening of particles at sampling pores and thus the objective of the numerical phase of our work is to determine whether lateral migration can be used to predict sample concentrations *a priori*.

The fluid that flows along a wall into a pore forms a tunnel-like shape called a capture tube by Tutty (1988). The boundaries of this capture tube are formed by so-called limiting streamlines. If a limiting streamline is less than one sphere radius from the wall, any contribution to the sample made by a sphere will be lost. This is an additional screening mechanism and is referred to as steric exclusion in this work. It is also to be taken into account in the numerical simulations.

## Experiment

The experiment is designed to permit variation in sampling rate, pore diameter, and flow field. This is done in a baffled Rushton stirred tank, in which the fluid suspension is continuously stirred and samples are taken through a pore in the vertical cylindrical wall above the plane of the stirrer. A Rushton stirred tank was chosen so that good mixing could be assured and so that the results of previous flow studies could be used (Calabrese, 1986; Ekert et al., 1985).

The suspension contains a dilute, monodisperse suspension of neutrally buoyant ABS (acrilonitrile-butadiene-styrene) spheres 1.50 mm in diameter in a propanediol/glycerin (20:1 by vol) liquid mixture. The liquid viscosity is 63 mPa·s and its density is 1,050 kg/m$^3$. All experiments were conducted in a temperature-controlled room at $299 \pm 0.5$ K. Sphere sedimentation rates in a stagnant mixture were measured and kept below 0.01 mm/s by adjusting the relative glycerin content to ensure virtual neutral buoyancy. For most experiments, tank sphere concentration is 0.2 vol. % ($\phi_t = 0.002$). This concentration was chosen to be sufficiently low to eliminate particle–particle interactions and sufficiently high to provide good particle counts. According to Feuillebois (1989), when solids volume fractions are greater than 1%, two-body interactions occur. At $\phi_t = 0.002$, the motion of each particle is thought to be affected only by fluid-velocity gradients and hydrodynamic interactions with boundaries.

Figure 1 shows the tank dimensions. Fluid volume is 2.008 L, and the depth is 140 mm. There are four vertical baffles, 90° apart, which protrude 14 mm into the tank. The stirrer is a six-bladed Rushton impeller 48 mm in diameter and is one-third of the way from the tank bottom to the liquid level. When the impeller is turning, three distinct, flow cells are

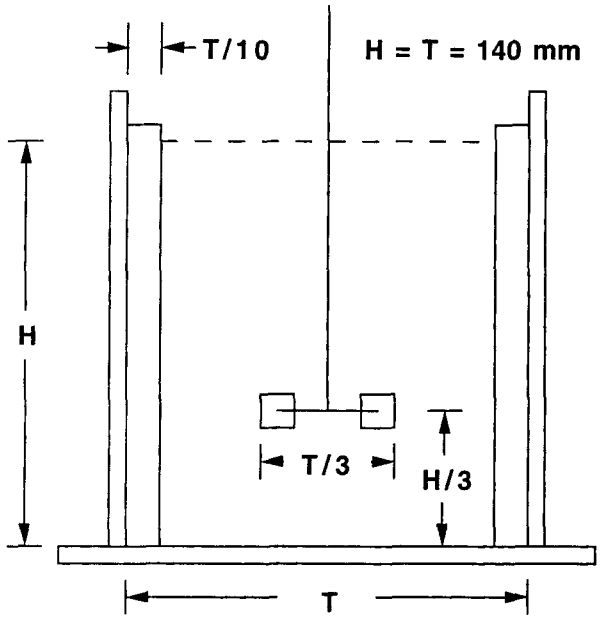


**Figure 1. Rushton-type stirred tank with a six-bladed impeller.**

The experimental tank has a fluid volume of 2.008 L.

established. A lower cell forms from the impeller to the tank bottom. A central flow cells sets up from the impeller toward the liquid level. There is also a small surface cell (see Figure 2). Only the vertical and radial velocity components are depicted; the angular velocities are not shown because they are negligible in the vicinity of the sampling pore, on account of the baffles. Pore centers are in a vertical plane midway between baffles and, in most cases, in a horizontal plane 33 mm above that of the impeller. Pores measure 3, 6 and 12 mm, or 2, 4 and 8 times the sphere diameter, respectively.

In most of the experiments in this study, the suspension approaches the sampling port by flowing upwards along the

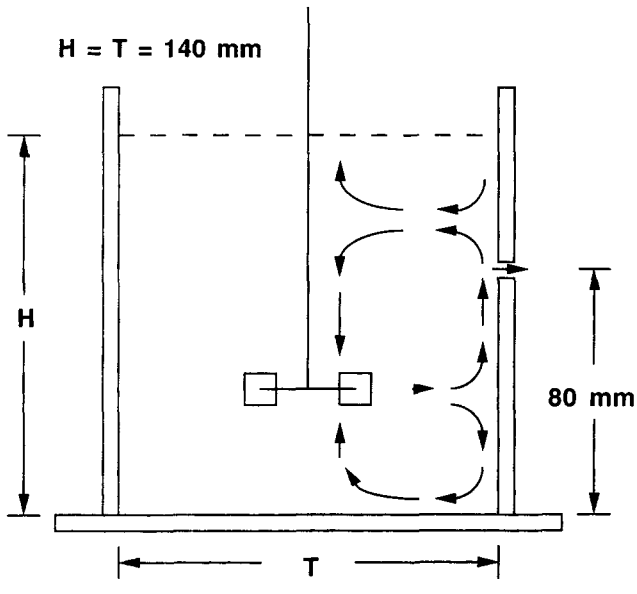


**Figure 2. Flow cells in a plane midway between baffles.**

A sampling pore is near the top of the central flow cell.

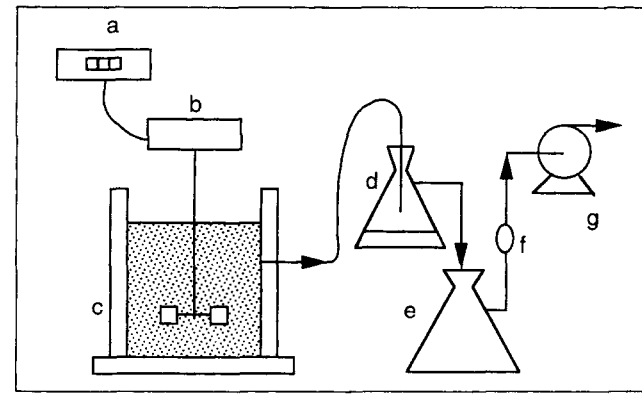


**Figure 3. Experimental system**

(a) RPM counter; (b) stirring motor; (c) Rushton-type baffled tank; (d) vacuum; (e) surge vessel; (f) scrubber; (g) peristaltic pump.

tank wall, with the pore located at a point before which the flow field begins to turn radially inward. Some of the suspension is sampled and the rest flows past. Streamlines separate fluid entering the pore from that excluded from the capture tube. When the impeller speed or the withdrawal velocity is varied, the size and shape of the capture tube changes.

Fluid is withdrawn from the tank through a pore with a flexible tube of the same diameter as the pore. The tubes are approximately 300 mm in length and empty into a collection flask. A variable-speed peristaltic pump allows the average velocity in the pore to be kept at 10 mm/s. An empty 2-L flask and a snubber (a cylinder of sintered metal) are placed in the line downstream of the collection flask to remove the pulsing action of the pump. The sampling system is shown in Figure 3.

Experimental stirrer speeds range from 100 to 500 rpm. According to laser Doppler measurements of Costes and Couderc (1988), the shape and size of the flow cells remain the same as the stirrer speed increases. Only the magnitudes of the velocities change (in proportion to stirrer speed change). Accordingly, impeller tip speed is used as the characteristic velocity of the suspension.

Sample volumes range from 0.05 to just over 0.1 L, or less than 5% of the total fluid volume. Samples much larger than 0.1 L may affect the size and shape of the central flow cell. Each sample is withdrawn, analyzed by weighing and counting the particles, and returned to the tank before the next experiment is conducted. For any given stirring speed and sample withdrawal velocity, concentrations vary from sample to sample. Therefore, four to six samples are taken for each flow condition and averaged.

## Theory

To predict the concentration of the suspension sample entering the pore, we consider two mechanisms: lateral migration (or lift-out) and steric exclusion. The lift-out mechanism is handled by incorporating the results of Schonberg and Hinch (1989) in a computation of lateral migration of particles out of the capture tube. The steric exclusion mechanism is handled by computing a flow-average contribution of the "outside" portions of the capture tube where all sphere cen-

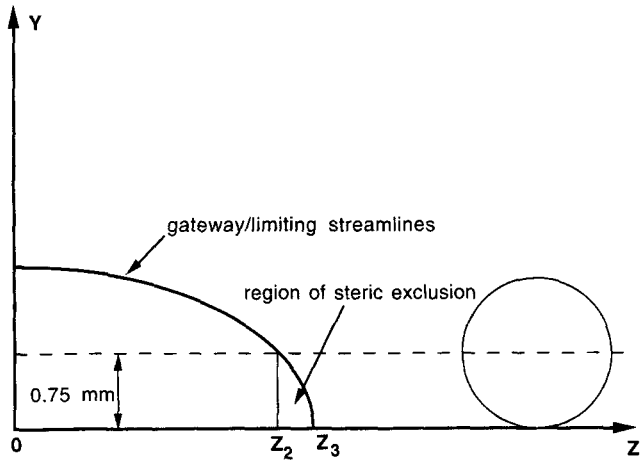


**Figure 4. Section of the gateway between $Z = Z_2$ and $Z = Z_3$ and $Y = 0.75$ mm is a region of steric exclusion.**

No sphere centers can enter here. All solids contributions to this region will be screened.

ters are always beyond the limiting streamlines and are thus screened geometrically (see Figure 4). This requires that the limiting streamline be less than one sphere radii from the wall. As the fluid velocity along the wall increases (or the fluid velocity in the pore decreases), the limiting streamlines, and hence the entire capture tube, becomes smaller. This causes $Z_2$ in Figure 4 to move closer to $Z = 0$. For a small enough capture tube, *all* spheres ($\Phi_s = 0$) will be screened by steric exclusion.

Segre and others conclude that the inertia of the fluid and the presence of a rigid wall must be responsible for the tubular pinch effect. Schonberg (1986) describes the effect as being a balance of two forces. One is created by the sphere's interaction with the wall and its neighboring shear field, causing a migration away from the wall. The other is created by the shear and curvature of the Poiseuille flow, causing a migration away from the centerline. These two opposing forces depend on radial position and balance at approximately $0.6R$, where $R$ is the tube radius.

An equivalent pinch effect also exists for parabolic flow between flat plates (Schonberg, 1986; Otis et al., 1986). It follows that a type of pinch effect would also be found in a viscous suspension flow with a curved velocity profile near a single flat wall. For our apparatus, sphere diameters are approximately two orders of magnitude smaller than the tank diameter, so the particles can be thought of as flowing along a flat wall, thereby permitting us to use the predictions of Schonberg quantitatively.

Figure 5 shows a semi-infinite fluid with a curved velocity profile flowing near a flat wall containing a pore through which fluid is being withdrawn. There must exist a limiting streamline such that the fluid flowing between it and the wall will enter the pore. If the fluid is a dilute suspension of spheres, a sphere flowing parallel to a wall will also migrate laterally away from it. This migration will cause the sphere to cross streamlines. A sphere located just on the wall side of the limiting streamline may eventually migrate through. Therefore, if a suspension flowing along a wall is being sampled through a pore, some spheres may be lost due to lateral migration through the limiting streamline, causing the sample to be deficient in solids.

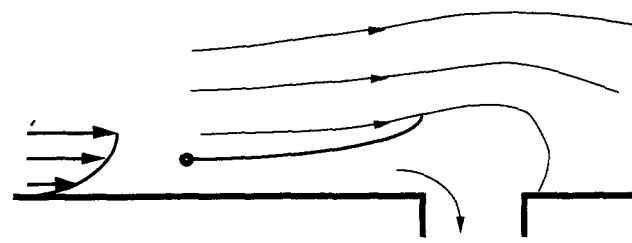

**Figure 5. Limiting trajectory.**

All spheres entering the capture tube between the limiting trajectory and the wall will enter the pore. Spheres within the limiting streamline and outside the limiting trajectory are lost from the sample due to lateral migration.

All spheres flowing in the neighborhood of a wall will migrate away from the wall but not all will be lost from the sample. There will exist a limiting trajectory (see Figure 5 again), such that all spheres that enter the capture tube between it and the wall will be captured and all those that enter above it will be lost from the capture tube. We refer to this particle screening procedure as the lift-out mechanism.

The lateral migration velocities of neutrally buoyant spheres in dilute suspensions in Poiseuille flow between flat plates were calculated by Schonberg and Hinch (1989). These migrations were calculated for a channel Reynolds number range of 1 to 150. This is within the experimental range of Segre and Siberberg, and also within our experimental range. Schonberg's lateral velocities are used to predict sphere trajectories in the computer simulations. An *a priori* calculation of sample concentration can be made if limiting streamlines and limiting trajectories are known in three dimensions.

In order to apply the results of Schonberg and Hinch, it is necessary to know the velocity field around and upstream of the pore. This was accomplished by numerical solution for the region of the top of the central flow cell, using the FIDAP computer code, Version 4.15, published by Fluid Dynamics International of Evanston, Illinois. This code solves the Navier–Stokes equations using a finite-element method.

The boundaries of the flow system that is simulated are shown in Figure 6. According to laser Doppler measurements of Costes and Couderc (1988), and our own laboratory observations, the flow in this region is virtually vertical. Therefore, the flow in the region of simulation can be represented by a series of two-dimensional slices. Also, since tank Reynolds numbers are calculated (as in Hiraoka et al., 1988) to be 59 for 100 rpm to 295 to 500 rpm, the flow region near the wall is considered to be laminar. The velocities along boundaries (1) and (2) of Figure 6 are taken from the measurements of Costes and Couderc. The velocities on boundary (3) are left variable. A parabolic profile is prescribed along boundary (4), which is the exit from the pore. No-slip conditions are imposed along solid boundaries. Solutions are obtained for a succession of two-dimensional sections of the capture tube in order to reduce computation time relative to three-dimensional computation. Each section is a plane containing fluid streamlines and lines parallel to the pore axis. For a given pore size, each section will contain a different size pore entrance, as seen by the moving fluid. Errors introduced by ne-

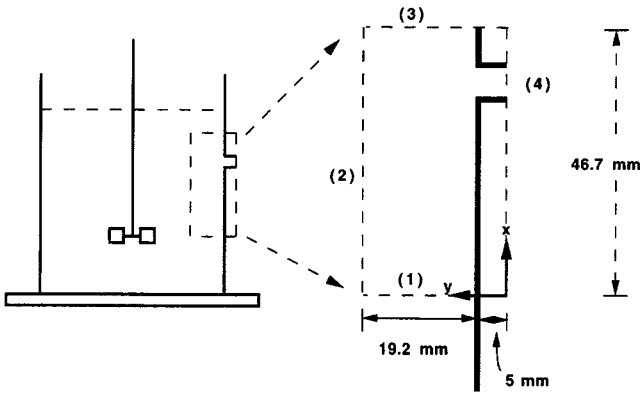


**Figure 6. Boundaries of the computer simulation.**

The velocity measurements of Costes and Couderc are used for the boundary conditions along (1) and (2). The velocities along (3) are variable. A parabolic velocity profile is prescribed at the exit of the pore (4).

glecting cylindricity are small, since the height of a section is small compared to the tank radius. Velocities perpendicular ($z$-component) to these two-dimensional sections are assumed to be negligible. According to Tutty (1988), for slow withdrawal velocity, these effects are small and we neglect them in this work.

Once the velocity field is found, it is simple to identify the streamline that forms the boundary of the capture tube for the liquid. The task then becomes one of determining the particle trajectory that reaches this capture tube just at the entrance to the pore. The starting point for this trajectory is within the capture tube well upstream of the pore (approximately 20 sphere diameters). The particle trajectory is computed using the relationship of Schonberg and Hinch (1989). Lift velocities are given as a function of distance from the wall. We superimpose these lift velocities onto the fluid velocities calculated previously to obtain particle trajectories.

The limiting streamlines and limiting trajectories for the several sections are then analyzed to calculate sample concentrations. This procedure amounts to a numerical integration over the various sections so that the entire pore area is included.

Certain assumptions are included in these numerical simulations:

1. There is no lateral migration directly over a pore (i.e., without a wall). Although there is undoubtedly some lateral migration in an "unbounded" flow (see Saffman, 1965), we assume here it is small compared to that caused by a wall. Therefore, as soon as the sphere is no longer flowing along a wall and is directly over a pore, it simply flows along the fluid streamline into the pore.

2. There are no particle–particle interactions. Since these simulations deal only with very dilute suspensions ($\phi_t$ = 0.002), it is assumed that the particles are far enough apart to behave independently. Assuming a face-center cubic array, the interparticle gap is 10.79 sphere radii.

3. It is the sphere center that is either captured or lost from the sample. If a sphere center is on the wall side of the limiting streamline and then migrates across it, it is assumed that the sphere is lost from the sample (even though part of that sphere may remain on the wall side as it passes over the pore). Also, of course, if the sphere center is captured, then the whole sphere is captured.

4. It is assumed that the suspension enters the capture tube as a "true" sample (where $\phi = 0.002$). Sphere centers are statistically equally likely to exist at any point in a well-mixed system. However, no sphere center can be closer to a wall than one radius (0.75 mm). Therefore the sphere centers (at the entry to the capture tube), which statistically would otherwise exist closer to the wall than one radius, are assumed to be pushed or placed in a position 0.75 mm from the wall. These spheres proceed from this placement. Some spheres are sterically excluded at this point.

5. Brownian motion is negligible, owing to the large size of the particles and the high viscosity of the fluid.

All computer programs are written to determine the liquid velocity field designated in Figure 6. These programs yield two-dimensional solutions and correspond to laminar, steady-state flow. The FIDAP code solves the Navier–Stokes equations using successive substitutions. The linear solution (the creeping-flow equation) is solved as a first guess for the nonlinear Navier–Stokes problem. These programs typically require 3 to 5 min CPU time on an IBM 3090 to converge to a relative velocity error of 1%. This occurs in three to seven iterations, depending on impeller speed.

Computed velocity fields exhibit curved velocity profiles near the wall. These profiles are parabolic in $v_x$ (the velocity parallel to the wall) from the wall up to a maximum velocity. Beyond the maximum velocity, the flow is complicated and not parabolic, but this does not concern us, since all of the capture tubes in this work lie between the wall and the position of maximum $v_x$. Figure 7 shows the velocity profile at a position 20 mm upstream of the pore. This is for the case of a 3-mm pore and a 100-rpm stirring speed. The maximum velocity is 5.92 cm/s at $Y_m$ = 7.2 mm. Up to $Y_m$, all velocities in this study are parabolic to within approximately 2%.

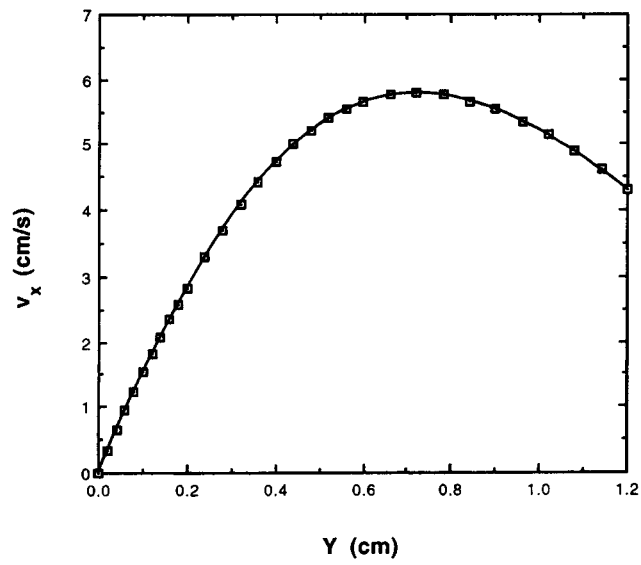


**Figure 7. Velocity profile at a position 20 mm upstream from the 3-mm pore located at the top of the central flow cell with a stirring speed of 100 rpm.**

The maximum velocity is 5.79 cm/s at $Y_m$ = 7.2 mm.

As the fluid enters the capture tube, the perpendicular velocity component $v_y$ is very small compared with $v_x$. However, as the fluid travels upward along the wall, away from the impeller plane, it slows down and begins to circulate back into the center of the tank. This causes $v_y$ to grow and $v_x$ to diminish, resulting in an expansion of the capture tube, since the limiting streamlines move away from the wall. This is shown in Figure 5. This is also due to the presence of the pore. The limiting streamline bows out well over the pore and ultimately attaches to the tank wall just beyond the pore. These general features have been shown in related flows both experimentally (Rong and Carr, 1990) and in computer simulation (Tutty, 1988). Also, as stirrer speed increases, the limiting streamlines move closer to the wall (provided pore withdrawal velocity remains constant).

The maximum velocity parallel to the wall ($v_{x,m}$) moves away from the wall as the fluid travels up and away from the impeller plane. This maximum velocity was used in the calculation of a channel-type Reynolds number. The distance from the wall to the position of $v_{x,m}$ was doubled and used as a "channel" width, so that $Re_c = 2Y_m v_{x,m}/\nu$. Here, $Re_c$ = channel Reynolds number; $Y_m$ = distance from the wall to the maximum velocity parallel to the wall; $v_{x,m}$ = the value of the maximum velocity parallel to the wall; and $\nu$ is the kinematic viscosity of the propanediol/glycerin solution. $Re_c$ is used as part of the calculation of lift velocities for the suspended spheres (Schonberg and Hinch, 1989).

Since the fluid slows down as it flows through the capture tube, and $v_{x,m}$ and $Y_m$ change with position, a channel Reynolds number must be calculated at every point to compute lift velocities. Channel Reynolds numbers ranged from 10 to 50.

Figure 5 shows, in two dimensions, both the limiting streamline and the limiting trajectory. Given the complete graphical numerical solution with depictions of streamlines, the limiting streamline, defining the fluid's capture tube, is immediately obvious. The particle's limiting trajectory, which is normally located within the limiting streamline, is determined by an iterative procedure. At the gateway to the capture tube, an imaginary sphere is located at some point between the wall and the limiting streamline. Based upon fluid properties, particle size and position, and velocity field, the lift velocity of a sphere can be computed from Figure 2 of Schonberg and Hinch (1989). This lift velocity allows one to calculate the new position of the particle, relative to the fluid streamline, as it moves downstream an incremental distance toward the pore (slot, in two dimensions). At the end of this step, a new velocity is computed and the calculational process is repeated. Nine steps in the $x$-direction were used, with size increments decreasing from 3.2 mm to 1.5 mm as the fluid moved toward the pore. Ultimately, the pore is reached and one can readily determine whether or not the sphere is captured. If the sphere is captured, the initial starting point on the gateway face of the capture tube is moved away from the wall and the entire series of calculations is repeated, until the particle streakline is established where the sphere barely escapes the pore. This procedure could be used to determine the vertical position of the limiting trajectory with a precision of 0.1%.

The computer program yields a two-dimensional solution. In order to simulate the three-dimensional case, several of these solutions were combined. That is, the three-dimensional capture tube is created by assembling several "slices" along the tube. The limiting streamlines of these slices taken together forms the capture tube. This capture tube shrinks as fluid flows faster (higher rpm) at constant pore withdrawal velocity. At the entrance to the capture tube is an archlike shape or gateway. Calculations of sample concentrations are made from limiting streamline and limiting trajectory information at this gateway.

Consider two-dimensional parabolic flow along a wall toward a pore. As part of this fluid is pulled into the pore, there exists a limiting streamline separating fluid entering a pore from that flowing by, forming a capture tube. The starting point ($X = 0$, $Y = \beta$) is somewhat arbitrary in terms of the $x$-distance, but is chosen to be sufficiently large that negligible lift occurs before this point. All fluid entering between ($X = 0$, $Y = 0$) and ($X = 0$, $Y = \beta$) flows into the pore. If this fluid contains neutrally buoyant particles, there will exist a limiting trajectory for these particles that begins at ($X = 0$, $Y = \alpha$), where $\alpha < \beta$. The fraction of the suspension entering between $Y = \alpha$ and $Y = \beta$ will lose all of its spheres due to lift.

We define an exclusion function, $f$, as the flow average of the fluid entering the capture tube that loses its particles from the tube due to lift:

$$f = \frac{\int_{\alpha}^{\beta} U(Y)_{x=0}\, dY}{\int_{0}^{\beta} U(Y)_{x=0}\, dY}. \tag{2}$$

Only the $x$-direction velocity component ($U(Y)$) is used for the entry plane ($x = 0$) because the $y$-component is negligible there.

A three-dimensional calculation is accomplished by performing a series of two-dimensional solutions of varying "pore" or slot width and numerically intergrating these over the total pore. Velocity components perpendicular to the two-dimensional plane are neglected. Axisymmetric parabolic profile into the pore is assumed:

$$v_m(\rho) = v_{m,0}(1 - \rho^2), \tag{3}$$

where $v_m(\rho)$ is the maximum velocity of a slot at $\rho$, the fractional distance from the pore center to the lateral edge of the pore oriented in the $z$-direction; $v_{m,0}$ is the maximum velocity of the central slot and $0 \le \rho \le 1$. At $\rho = 0$ (the central slot solution), flow into the pore and hence into the gateway, is at its maximum. Parabolic flow into the 2-dimensional pore (or slot) means that the average velocity is half $v_m(\rho)$. As $\rho$ approaches unity, the flow goes to zero. $v_m(\rho)$ is prescribed as a boundary condition for each (FIDAP) slot solution.

The total flow into the pore (and hence the gateway) as a function of $\rho$ is

$$\int_0^1 v_m(\rho) L(\rho)\, d\rho, \tag{4}$$

where $L(\rho)$ = is a geometric weighting factor ranging from 1 to 0 as $\rho$ goes from 0 to 1, defined by

$$L(\rho) = (1-\rho^2)^{1/2}. \tag{5}$$

Combining Eqs. 3, 4 and 5, the total flow into the gateway can be represented as

$$v_{m,o}\int_0^1 (1-\rho^2)^{3/2}\, d\rho. \tag{6}$$

Similarly, the fraction of flow entering the gateway between the limiting surface and the limiting trajectories is

$$\frac{\int_0^1 f(\rho)\, v_m(\rho) L(\rho)\, d\rho}{\int_0^1 v_m(\rho) L(\rho)\, d\rho}, \tag{7}$$

where $f(\rho)$ is the exclusion function of Eq. 2 expressed as a function of $\rho$.

Equation 7 can now be applied to calculations of overall particle concentration. Referring to Figure 8, flow entering region (a) has its particles captured, while the flow entering regions (b) and (c) lose all theirs. In region (c), between $Z_2$ and $Z_3$, no spheres can be captured since the sphere centers are excluded from the gateway, *steric exclusion*. The bulk of our computational effort has been the determination of the limiting trajectory for the region $0 < Z < Z_1$ and the calculation of the relative amount of flow entering region (a) of the gateway.

Therefore Eq. 7 can be rewritten as

$$1 - \frac{\phi_s}{\phi_t} = \frac{\int_0^{z_1} f(\rho) v_m(\rho) L(\rho)\, d\rho + \int_{z_1}^{z_3} v_m(\rho) L(\rho)\, d\rho}{\int_0^{z_3} v_m(\rho) L(\rho)\, d\rho}. \tag{8}$$

The righthand side of Eq. 8 is the fraction of spheres lost from the sample, where $Z_3$ is equivalent to $\rho = 1$. Equation 8 is used to calculate the predicted values of $\Phi_s$, which appear in Figure 12.

From Figure 8 and Eq. 8, as stirring speed increases, the capture tube gateway shrinks. Both $Z_1$ and $Z_2$ move toward the origin. Both mechanisms contribute to particle loss, and there will be a finite stirring speed at which $\Phi_s$ will reach zero. Increasing the speed further will decrease the gateway height at the origin until the height reaches one sphere radius. At this point, all the particles will be screened solely due to steric exclusion.

Full three-dimensional computer simulations by Tutty (for a somewhat simpler flow) have gateway shapes that are somewhat wider, with streamline attachments just beyond the radius of the pore. However, at low pore withdrawal velocities, differences between Tutty's results and those of this work are minimal.

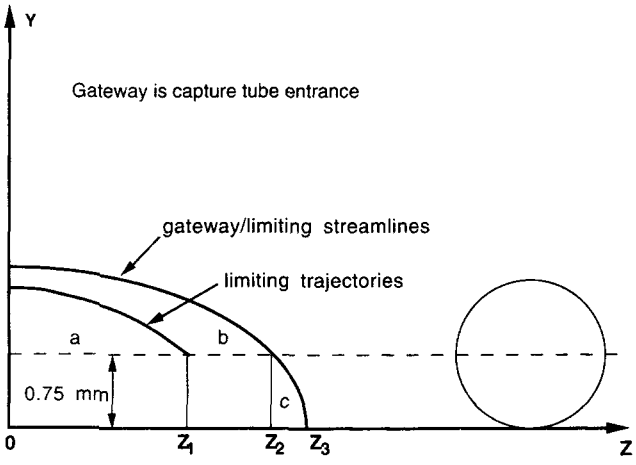


**Figure 8. Gateway to a capture tube.**

All sphere centers that enter region (a) are captured; all that enter region (b) are lost due to "lift-out." All contributions by spheres to the solids concentrations of region (c), provided the sphere center is between $Z_2$ and $Z_3$, are lost due to steric exclusion.

## Results and Discussion

### *Experiment*

Figure 9 shows that $\Phi_s$ decreases as the characteristic suspension velocity, $V_{ch}/V_s$, increases, $V_{ch}$ consists of the impeller tip speed, $\pi(T/3)\Omega$, and the $V_s$ is simply average pore velocity, $v$. Each point represents an average of four to six samples and has a standard deviation as shown by error bars. [For details see Jones (1991).] The sphere volume fraction of the sample is $\phi_s$ and the tank volume fraction is $\phi_t = 0.002$.

In general, as velocity ratio increases, sample concentrations decrease. Particle screening is found to be highly sensitive to velocity ratio. For example, for a 3-mm pore with a withdrawal velocity of 1 cm/s and an impeller rotation of 500 rpm (a velocity ratio in Figure 9 of about 140), over 90% of the particles are screened from the sample. Only about 10% are screened at 100 rpm for the same withdrawal velocity (a velocity ratio in Figure 9 of about 28). The screening effect is also found to be very sensitive to pore size: the smaller the pore, the greater the effect. Fahraeus found a similar de-

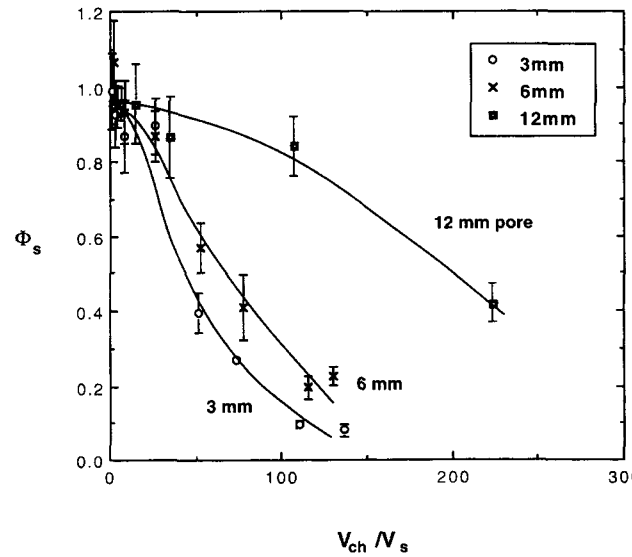


**Figure 9. Effect of pore size on sample concentration when $\phi_t = 0.002$.**

Pore position is at the top of the central flow cell.

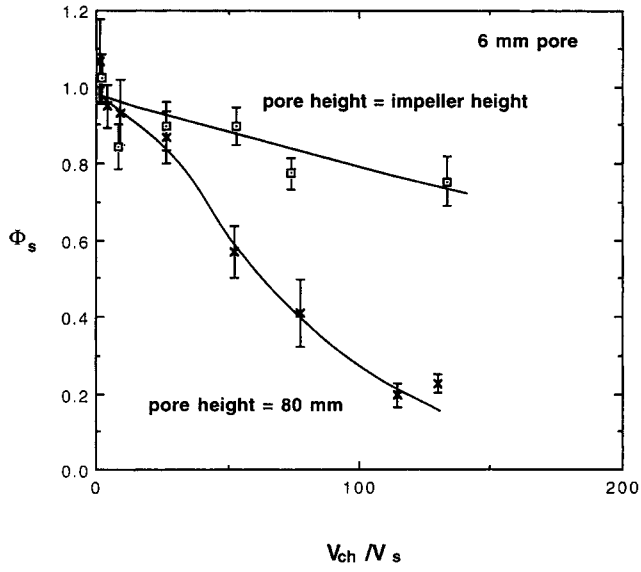


**Figure 10. Effect of pore location on sample concentration when $\phi_t = 0.002$.**

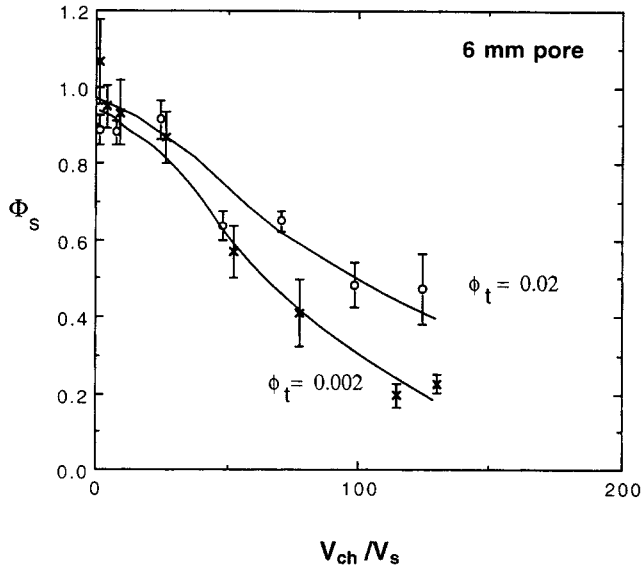


**Figure 11. Effect of tank concentration on sample concentration.**

Pore position is at the top of the central flow cell.

pendence on pore size, although for systems of much higher solids fraction ($\phi_t = 0.28$, 0.405).

For the experiments shown in Figure 9, the pore position near the top of the central flow cells causes the suspension to travel just over 30 mm (about 20 sphere diameters) along the wall to the sampling orifice.

Additional experiments were performed to show what happens when the pore is placed in the horizontal plane of the impeller and midway between baffles, Figure 10. The suspension does not flow along a wall before being sampled. Although the general trend of decreasing $\Phi_s$ with increasing impeller speed remains, the dependence is far weaker than that of Figure 9, with a 6-mm pore at the top of the central flow cell. With pore size and velocity ratio held constant, up to three times as many particles are screened when the pore location is 20 particle diameters away from the impeller plane.

Thus far, all experiments were conducted using highly dilute suspensions in order to avoid particle–particle interactions. A study was performed at a tenfold higher concentration, 2 vol. %, to see what effect, if any, particle–particle interactions might have on sample concentration. Results are shown in Figure 11 for samples taken with a 6-mm pore near the top of the central flow cell. At moderate to high velocity ratios, *fewer* spheres are screened from samples taken from the 2 vol. % solution. Evidently two-body interactions have occurred.

### *Discussion of experimental results*

A major purpose of our experiments was to establish the effects of the flow field and pore size on the sample concentration. It was found that pore diameter, stirring speed, withdrawal velocity, and pore location each can affect sample concentration significantly.

All of the experimental trends may be explained by the lift-out mechanism. For a given pore withdrawal velocity, as stirring speed increases, limiting streamlines move closer to the wall and the capture tube shrinks. Also, the closer a particle is to a wall, the higher the lateral migration velocity (Schonberg, 1989). It follows that at higher stirring speeds, a sphere is more likely to lift out of the capture tube, causing the sample to be deficient, as in Figure 9.

When a suspension flows directly from the impeller toward a pore, some spheres are screened, as shown in Figure 10. However, this screening effect is far smaller than for suspensions, which flow along a wall and are then sampled. Clearly, hydrodynamic interactions with a wall resulting in particles lifting out of a capture tube creates this dramatic difference.

The behavior of systems with the relatively high tank volume fraction of 2% ($\phi_t = 0.02$, as shown in Figure 11) is somewhat more complicated. Here we must first consider the gap between particles. Assuming a cubic array, the interparticle gap is $(4/3\pi a^3/\phi)^{1/3} - 2a$, where $a$ is the sphere radius. This gives a gap of 10.79 for $\phi_t = 0.002$ and 3.94 for $\phi_t = 0.02$. If the particles are far enough apart (as in a very dilute solution), they behave as if in isolation (as has been assumed for $\phi_t = 0.002$). That is, they may migrate through the limiting streamline unimpeded by neighboring particles. At a much higher concentration, a particle's lateral migration can be slowed down by another particle, more distant from the wall, which is in the closer particle's migration path. This more distant particle is moving away from the wall more slowly or possibly not migrating at all. This migration hindrance will cause some particles to remain in the capture tube that otherwise would have migrated out. Samples taken at relatively high tank concentrations are then expected to have a *smaller* deficiency (a higher $\phi_s/\phi_t$) in the sample than for highly dilute tank concentrations. This is observed experimentally and shown in Figure 11.

### *Simulation results and discussion*

Figure 12 contains experimental results and predictions for

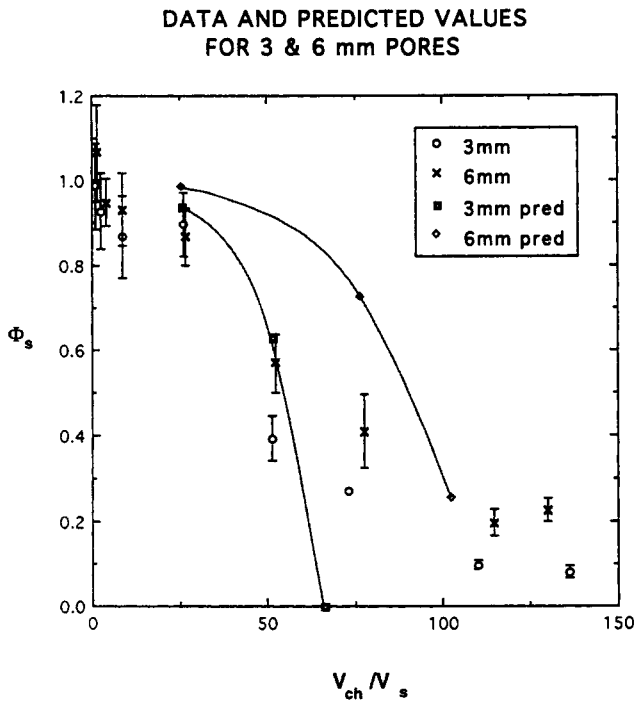


**Figure 12. Experimental results and predictions for 3-mm and 6-mm pore sampling.**

sample concentrations obtained with 3-mm and 6-mm pores located at the top of the central flow cell taken from dilute ($\phi_t = 0.002$) suspensions. The experimental data follow an inverted S shape, with virtually true samples obtained at low velocity ratio, followed by a rapid decline in sample concentration, and finally, at high velocity ratios, there is a leveling-off or "tail" with very low sample concentrations.

The theoretical predictions are quite close (within about 10 to 20%) for the 3-mm pore case at low to moderate velocity ratios. For the larger pore diameter, the predicted sample concentration falls off with velocity ratio somewhat later than observed experimentally, although the trend is certainly correct, and the sharpness of the dependence is matched. At higher velocity ratios, the predictions fall toward zero, and do not exhibit the gradual horizontal asymptote. This may be caused by our having exceeded the Reynolds numbers for which the scheme is valid. Schonberg's relationship was obtained for channel Reynolds numbers ranging from 1 to 15, whereas our equivalent *Re* is 50 at 400 rpm. Further, as Reynolds number (velocity) increases, Segre and Silberberg and Schonberg and Hinch found that the equilibrium point for the particles moves closer to the wall, implying less lift at higher *Re*. Therefore, at higher stirring speeds (velocity ratio), the simulations predict lift velocities that are probably too large, causing the predictions to fall off a bit too rapidly with velocity ratio.

For the range of variables in this study, simulations show that lift has a greater effect than steric exclusion, as shown in Table 1. Lift becomes relatively more important, as the fluid flows by the pore faster (higher rpm) with constant withdrawal velocity. This makes sense, since the capture tube shrinks closer to the wall at higher rpm, and less lateral distance need be traveled by a sphere to escape capture. Also lateral velocities are higher nearer the wall.

**Table 1. Screening Mechanisms vs. Simulation Results**

| Pore Size mm | rpm | Fraction of Spheres Entering Capture Tube Lost by: Lift | Steric Exclusion | $\Phi_s$ by Simulation |
|---|---|---|---|---|
| 3 | 100 | 0.04 | 0.03 | 0.93 |
| 3 | 200 | 0.25 | 0.13 | 0.62 |
| 6 | 100 | 0.01 | 0.01 | 0.98 |
| 6 | 300 | 0.18 | 0.08 | 0.74 |
| 6 | 400 | 0.56 | 0.20 | 0.25 |

Under certain circumstances, it is possible that $\Phi_s > 1$. This is consistent with theory. When the capture tube extends beyond the equilibrium point but is still inside the position of maximum velocity, there will be lateral migration into the capture tube (lift-in) due to the tubular pinch effect. The solids in the sample are thereby enhanced. For example, in central slot solution, for low rpm, some lift-in was calculated along with some steric exclusion, which added to $\Phi_s$ of about one.

## Conclusions

Samples taken of a stirred fluid suspension through a pore in a wall contain fewer particles than the bulk suspension. The normalized concentration $\Phi_s$ decreases from unity nearly to zero with increased stirring speed and decreased pore size.

*A-priori* predictions of $\Phi_s$ are obtained by calculating the degree of particle screening from mechanisms of steric exclusion and inertial migration, or lift-out. Inertial migration, the more significant mechanism in the present work, is based on the work of Schonberg and Hinch (1989), who calculated lift velocities for a freely rotating sphere in a fluid undergoing parabolic flow between parallel plates. In the present geometry the flow upstream of the pore is similar, nearly parabolic, and nearly parallel to the wall; particles move away from the wall as the fluid travels toward the pore. For $\Phi_s = 0.5$, agreement between experimental and predicted characteristic velocities is quite good—within 20% for a 6-mm pore and within 5% for a 3-mm pore. Additional support for the inertial migration mechanism comes from samples taken through a pore in the plane of the impeller, or one in which there is no parallel flow along a wall upstream of the pore. Far fewer particles are screened out, presumably because the particles do not experience hydrodynamic interactions with a wall.

Experiments were also conducted using a suspension with a tenfold higher sphere concentration (2 vol. %) to investigate the effect of particle–particle interaction. At higher concentration, fewer spheres are screened. This difference is shown to be consistent with the lateral migration mechanism.

## Notation

$H$ = tank height
$L(\rho)$ = geometric weighting factor
$T$ = tank height
$V_s$ = sampling velocity
$\alpha$ = starting distance from tank wall for limiting trajectory
$\beta$ = starting distance from tank wall for limiting streamline
$\Omega$ = impeller speed

## Literature Cited


Altena, F. W., and G. Belfort, "Lateral Migration of Spherical Particles in Porous Flow Channels: Application to Membrane Filtration," *Chem. Eng. Sci.*, **39**, 343 (1984).

Berge, L. I., "Radial Migration of a Single Particle in a Pore by the Resistive Pulse and the Pressure Reversal Technique," *J. Fluid Mech.*, **217**, 349 (1990).

Bauser, H., H. Chmiel, N. Stroh, and E. Walitza, "Interfacial Effects with Microfiltration Membranes," *J. Memb. Sci.*, **11**, 321 (1982).

Bretherton, F. P., "The Motion of Rigid Particles in a Shear Flow at Low Reynolds Number," *J. Fluid Mech.*, **14**, 284 (1962).

Calabrese, R. V., T. P. K. Chang, and P. T. Dang, "Drop Breakup in Turbulent Stirred-tank Contactors, Part 1. Effect of Dispersed-phase Viscosity," *AIChE J.*, **32**, 657 (1986).

Cokelet, G. R., *Microcirculation*, Vol. 1, J. Grayson and W. Zingg, eds., Plenum, New York (1976).

Costes, J., and J. P. Couderc, "Study by Laser Doppler Anemometry of the Turbulent Flow Induced by a Rushton Turbine in a Stirred Tank: Influence of the Size of the Units-1. Mean Flow and Turbulence," *Chem. Eng. Sci.*, **43**, 2751 (1988).

Cox, R. G., and H. Brenner, "The Lateral Migration of Solid Particles in Poiseuille Flow," *Chem. Eng. Sci.*, **23**, 147 (1968).

Dagan, Z., S. Weinbaum, and R. Pfeffer, "An Infinite-series Solution for the Creeping Motion Through an Orifice of Finite Length," *J. Fluid Mech.*, **115**, 505 (1982).

Dagan, Z., S. Weinbaum, and R. Pfeffer, "General Theory for the Creeping Motion of a Finite Sphere along the Axis of a Circular Orifice," *J. Fluid Mech.*, **117**, 143 (1983).

Eckert, R. E., C. M. McLaughlin, and J. H. Rushton, "Liquid-Liquid Interfacial Areas Formed by Turbine Impellers in Baffled, Cylindrical Mixing Tanks," *AIChE J.*, **31**, 1811 (1985).

Fahraeus, R., "The Suspension Stability of Blood," *Physiol. Rev.*, **9**, 241 (1929).

Feuillebois, F., "Some Theoretical Results for the Motion of Solid Spherical Particles in a Viscous Fluid," *Multiphase Science and Technology*, Vol. 4, G. F. Hewitt, J. M. Delhaye and N. Zuber, eds., Hemisphere, p. 583 (1989).

Gaehtgens, P., "Flow of Blood Through Narrow Capillaries: Rheological Mechanisms Determining Hematocrit and Apparent Viscosity," *Biorheology*, **17**, 183 (1980).

Green, G., and G. Belfort, "Fouling of Ultrafiltration Membranes: Lateral Migration and the Particle Trajectory Model," *Desalination*, **35**, 129 (1980).

Hiraoka, S., I. Yamada, T. Aragaki, H. Nishiki, A. Sato, and T. Takagi, "Numerical Analysis of Three Dimensional Velocity Profiles of Highly Viscous Newtonian Fluid in an Agitated Vessel with Paddle Impeller," *J. Chem. Eng. Jpn.*, **21**, 79 (1988).

Ho, B. P., and L. G. Leal, "Inertial Migration of Rigid Spheres in Two-dimensional Unidirectional Flows," *J. Fluid Mech.*, **65**, 365 (1974).

Jones, F., "On the Sampling of Suspensions in Laminar Flow," PhD Diss., Dept. of Chemical Engineering, Drexel Univ., Philadelphia (1991).

Levesley, J. A., and B. J. Bellhouse, "Particulate Separation Using Inertial Lift Forces," *Chem. Eng. Sci.*, **48**(21), 3657 (1993).

Nasr-El-Din, H., and C. A. Shook, "Particle Segregation in Slurry Flow Through Vertical Tees," *Int. J. Multiphase Flow*, **12**(3), 427 (1986).

Otis, J. R., F. W. Altena, J. T. Mahar, and G. Belfort, "Measurements of Single Spherical Particle Trajectories with Lateral Migration in a Slit with One Porous Wall under Laminar Conditions," *Exp. Fluids*, **4**, 1 (1986).

Rong, F. W., and R. Carr, "Dye Studies on Flow Through Branching Tubes," *Microvasc. Res.*, **39**, 186 (1990).

Saffman, P. G., "The Lift on a Small Sphere in a Slow Shear Flow," *J. Fluid Mech.*, **22**, 385 (1965).

Schonberg, J., "The Hydrodynamics of Small Suspended Spheres with Application to Membrane Fouling," PhD Diss., Dept. of Chemical Engineering, Rensselaer Polytechnic Institute, Troy, NY (1986).

Schonberg, J., and E. Hinch, "Inertial Migration of a Sphere in Poiseuille Flow," *J. Fluid Mech.*, **203**, 517 (1989).

Segre, G., and A. Silberberg, "Radial Particle Displacements in Poiseuille Flow of Suspensions," *Nature*, **189**, 209 (1961).

Segre, G., and A. Silberberg, "Behavior of Macroscopic Rigid Spheres in Poiseuille Flow. Part 1. Determination of Local Concentration by Statistical Analysis of Particle Passages through Crossed Light Beams," *J. Fluid Mech.*, **14**, 115 (1962a).

Segre, G., and A. Silberberg, "Behavior of Macroscopic Rigid Spheres in Poiseuille Flow. Part 2. Experimental Results and Interpretation," *J. Fluid Mech.*, **14**, 136 (1962b).

Tutty, O. R., "Flow in a Tube with a Small Side Branch," *J. Fluid Mech.*, **191**, 79 (1988).

Vasseur, P., and R. G. Cox, "The Lateral Migration of a Spherical Particle in Two-dimensional Shear Flows," *J. Fluid Mech.*, **78**, 385 (1976).

Yan, Z., S. Weinbaum, and A. Acrivos, "Fluid Skimming and Particle Entrainment into a Small Circular Side Pore," *J. Fluid Mech.*, **229**, 1 (1991).



*Manuscript received Dec. 23, 1996, and revision received June 23, 1997.*